be exposed within this basin, they are likely mixed with other material (*19*).

The detection of a population of ancient, multiring basins with the altimetry data from Clementine has several implications for both the geological evolution of the moon and for our understanding of the other terrestrial planets. A variety of basin sizes, morphologies, and relative preservation states are evident in the altimetry data. This topographic information has confirmed and extended the detailed photogeologic mapping of the basins, which represent the fundamental topographical and structural features of the lunar crust. The confirmation that a large population of ancient basins exists in the lunar highlands strengthens arguments that the highlands are saturated with craters of very large diameter (*23*). A corollary of this observation is that at least the upper few kilometers to tens of kilometers of the lunar crust has been brecciated and mixed on scales of tens to hundreds of kilometers, confirming earlier suppositions (*1, 23*).

The amount of relief displayed by some of these features is astounding. Basins such as Mendel-Rydberg and South Pole–Aitken date back to the earliest stages of lunar history (some time between 4.3 to 3.9 billion years ago), yet they preserve relief indicating that very little relaxation of topography has occurred. Such preservation of relief suggests that attempts to date lunar basins by measuring the rim topography and the relative amounts of relaxation by viscous flow (*24*) probably are not valid. Near-isostatic compensation, as seen in basins such as Mendel-Rydberg (*7*), must have occurred nearly contemporaneously with the impact, probably in the form of the dynamic rebound and uplift of relatively dense mantle rocks during the modification stage of basin formation (*7, 25*).

The altimetry data from Clementine both confirm previously mapped basins and have led to the recognition of additional degraded structures. Thus, global topography is a valuable tool in the mapping of planetary surfaces. The confirmation of a large number of very degraded, ancient basins on the moon suggests that comparable photogeologic mapping of ancient basins on other terrestrial planets [summarized in (*2*)] probably has accurately depicted the configuration of these early crusts [compared to (*3*)]. Future missions to Mars and Mercury that carry instruments for the regional mapping of large-scale topography can help us decipher the early impact record of the crusts of these other terrestrial planets.

REFERENCES AND NOTES

1. D. E. Wilhelms, *U.S. Geol. Surv. Prof. Pap. 1348*, (1987). Old basins on the moon are named by identifying two unrelated, superposed craters that roughly outline the basin rim; thus, the Mendel-Rydberg Basin is named after the two much younger craters Mendel (49°S, 110°W; 138 km in diameter) and Rydberg (46.5°S, 96°W; 50 km in diameter). See D. E. Wilhelms and F. El-Baz, *U.S. Geol. Surv. Map I-948* (1977); D. E. Wilhelms, *NASA SP-469* (1984), pp. 107–205.
2. P. D. Spudis, *The Geology of Multi-ring Basins* (Cambridge Univ. Press, Cambridge, 1993).
3. H. J. Melosh, *Nature* **368**, 24 (1994).
4. E. A. Whitaker, *Proc. Lunar Planet. Sci. Conf.* **12A**, 105 (1981).
5. W. K. Hartmann and G. P. Kuiper, *Commun. Lunar Planet. Lab.* **1**, 51 (1962).
6. S. Nozette *et al.*, *Science* **266**, 1835 (1994).
7. M. T. Zuber *et al.*, *ibid.*, p. 1839.
8. W. K. Hartmann and C. A. Wood, *Moon* **3**, 3 (1971).
9. D. E. Wilhelms *et al.*, *U.S. Geol. Surv. Map I-1162* (1979).
10. P. H. Schultz and P. D. Spudis, *Proc. Lunar Planet. Sci. Conf.* **10**, 2899 (1979); *Nature* **302**, 233 (1983).
11. B. R. Hawke and J. F. Bell, *Proc. Lunar Planet. Sci. Conf.* **12B**, 665 (1981); R. Greeley *et al.*, *J. Geophys. Res.* **98**, 17183 (1993).
12. M. J. S. Belton *et al.*, *Science* **255**, 570 (1992).
13. B. K. Lucchitta, *U.S. Geol. Surv. Map I-1062* (1978).
14. B. N. Rodinov *et al.*, *Cosmic Res.* **9**, 410 (1971); *ibid.* **14**, 548 (1977).
15. D..E. Stuart-Alexander, *U.S. Geol. Surv. Map I-1047* (1978).
16. C. A. Wood and A. Gifford, in *Conference on Multi-ring Basins, Houston, Texas*, Lunar and Planetary Institute staff, Eds. (Elsevier, New York, 1981), pp. 121–123.
17. W. R. Wollenhaupt and W. L. Sjogren, *Moon* **4**, 337 (1972).
18. M. J. Bielefeld *et al.*, *Proc. Lunar Sci. Conf.* **7**, 2661 (1976); B. R. Hawke and P. D. Spudis, *Proceedings of the Conference on Highlands Crust* (Pergamon, New York, 1980) p. 467; P. A. Davis and P. D. Spudis, *Proc. Lunar Planet. Sci. Conf. 17, J. Geophys. Res. E* **92**, 387 (1987).
19. J. W. Head *et al.*, *J. Geophys. Res.* **98**, 17149 (1993).
20. P. G. Lucey *et al.*, Science **266**, 1855 (1994).
21. R. A. F. Grieve *et al.*, *Proc. Lunar Planet. Sci. Conf.* **12A**, 37 (1981).
22. S. K. Croft, *ibid.*, p. 207.
23. W. K. Hartmann, *Icarus* **60**, 56 (1984).
24. R. B. Baldwin, *ibid.* **71**, 1 (1987).
25. R. J. Phillips and J. Dvorak, *Proc. Lunar Planet. Sci. Conf.* **12A**, 91 (1981).

26. We thank the Ballistic Missile Defense Organization–Naval Research Laboratory Clementine Project for designing and flying a superb lunar mission, M. Zuber and D. Smith for providing copies of their processing of the Clementine altimetry data, and B. Fessler and S. Lee for image processing. We also thank B. R. Hawke and D. E. Wilhelms for helpful review comments. The participation of P.D.S. and J.J.G. on the Clementine Science Team is supported by National Aeronautics and Space Administration grant NAGW-3688. This paper is Lunar and Planetary Institute contribution 846.

2 August 1994; accepted 25 October 1994

The South Pole Region of the Moon as Seen by Clementine

E. M. Shoemaker,* M. S. Robinson, E. M. Eliason

The Clementine mission has provided the first comprehensive set of high-resolution images of the south pole region of the moon. Within 5° of latitude of the pole, an area of an estimated 30,000 square kilometers remained in shadow during a full lunar rotation and is a promising target for future exploration for ice deposits. The Schrödinger Basin (320 kilometers in diameter), centered at 75°S, is one of the two youngest, least modified, great multiring impact basins on the moon. A large maar-type volcano localized along a graben within the Schrödinger Basin probably erupted between 1 and 2 billion years ago.

A primary scientific objective of the Clementine mission was to map the spectral reflectance of the lunar surface at 11 wavelengths (*1*). Images taken above 70° latitude also reveal the lunar surface illuminated by the sun at angles that are ideal for discriminating subtle morphological features and thus for deciphering the stratigraphy and structure of the lunar surface. In this report, we present observations and interpretations of the geology of the south polar region, which was the least known part of the moon before the Clementine mission.

The highest resolution images of the south polar region were taken during the first 5 weeks of the mission. Nearly complete coverage between 70° and 90°S was obtained with the ultraviolet-visible (UV-VIS) camera during this period (Fig. 1). A broad swath of the terrain between 90° and 120°W longitude had never been satisfactorily observed and thus was essentially "luna incognita" on most existing lunar maps (*2*). Of particular interest is the area within 5° of the pole.

As the moon rotated during the first month of the Clementine mission, it became clear why a substantial area around the south pole is blank on global maps. A large fraction of this area, totaling an estimated 30,000 km^2, remains in shadow in the present phase of precession of the lunar pole (Fig. 1). Much of this shadowed area is part of an irregular topographic depression partly bounded on the sub-Earth side by high terrain known informally as the Leibnitz Mountains and, at westerly and easterly longitudes, by the high rims of several ancient large craters. It is possible that the depression coincides with a

E. M. Shoemaker, U.S. Geological Survey and Lowell Observatory, Flagstaff, AZ 86001, USA.
M. S. Robinson and E. M. Eliason, U.S. Geological Survey, Flagstaff, AZ 86001, USA.

*To whom correspondence should be addressed.

very ancient impact basin about 300 km in diameter whose outline has been largely obliterated by subsequent impacts. The Leibnitz Mountains may have been formed by the combined effect of uplift on the rim of this ancient basin and faulting and uplift on or near the rim of the still older and much larger South Pole–Aitken Basin (3, 4).

The polar regions of the moon are of special interest because of the postulated occurrence of ice in permanently shadowed areas (5); the south pole is of greater interest because the area that remains in shadow is much larger than that at the north pole. How much of this area is permanently shadowed during a full cycle of precession of the lunar poles is still to be determined and will require ground-based radar images of the south pole (5, 6) and future polar-orbiting missions. The south pole was the prime target for bistatic radar observations with Clementine, with the goal of searching for ice (1).

A feature of great geologic interest on the south polar mosaic (Fig. 1) is the Schrödinger multiring impact basin (320 km in diameter) centered at 138°E, 75°S (Figs. 1 and 2). This basin is the freshest, least modified lunar basin of its size. Previous work on the Schrödinger Basin was based on relatively low resolution oblique photographic images taken with the Lunar Orbiter 5 spacecraft (3, 7).

The Schrödinger Basin is defined by an outer ring, the topographic rim of the basin (Fig. 1). Clementine altimetry shows this basin to be ~2 to 3 km deep, rim to floor, reaching an elevation of −5 to −6 km on its floor (4, 8). The position of the rim crest along the southern and northern rim of the basin generally coincides with the outermost normal faults that bound the structural basin. A smooth-textured ejecta blanket extends hundreds of kilometers in all directions from the rim crest and reaches the permanently shadowed region of the south pole.

The inner ring of the basin is the peak ring, formed by uplift of pre-Schrödinger crustal materials (unit pr in Fig. 3), which constitute the oldest geologic unit exposed in the basin. Somewhat rectangular in outline, the peak ring consists of a discontinuous array of massifs. Linear structural elements bounding and within the massifs probably reflect pre-Schrödinger faults and fractures in the lunar crust. From theory, experiment, and extensive observations of terrestrial impact craters, the materials of central peaks are known to be derived from the floors of transient cavities excavated in the early stages of cratering events (9). At late stages, the floors rise to form central peaks concomitantly with the gravitational collapse of the transient cavity walls. In an impact crater as large as Schrödinger, the central part of the peak probably collapses and leaves an irregular central depression surrounded by the peak ring.

Basin wall material (unit bw in Fig. 3) is the next oldest geologic unit in the Schrödinger Basin. The unit bw consists of ejecta from the transient cavity that was dropped down the basin wall along a series of normal faults during cavity collapse. Huge landslides (labeled h in Fig. 3) cover the southwest wall of Schrödinger. These landslides overlap the basin wall material, but judging from the densities of superposed small craters on the landslides, they were emplaced soon after the formation of the basin. They occur where the wall of the Schrödinger Basin intersects the rim of the much older, subdued Amundsen-Ganswindt Basin (7), which is similar in size to the Schrödinger Basin (Fig. 1). The rim materials of the older basin evidently were susceptible to large-scale mass movement down the wall of the newly formed basin. The south rim of the older basin forms part of the high ground enclosing the shadowed region near the pole.

Units interpreted as shock-melted material are the most extensive geologic units in the Schrödinger Basin. Two facies are mapped in Fig. 3: a rough facies (unit rp), marked by gentle hummocks, swales, and low knobs typically a few kilometers across,

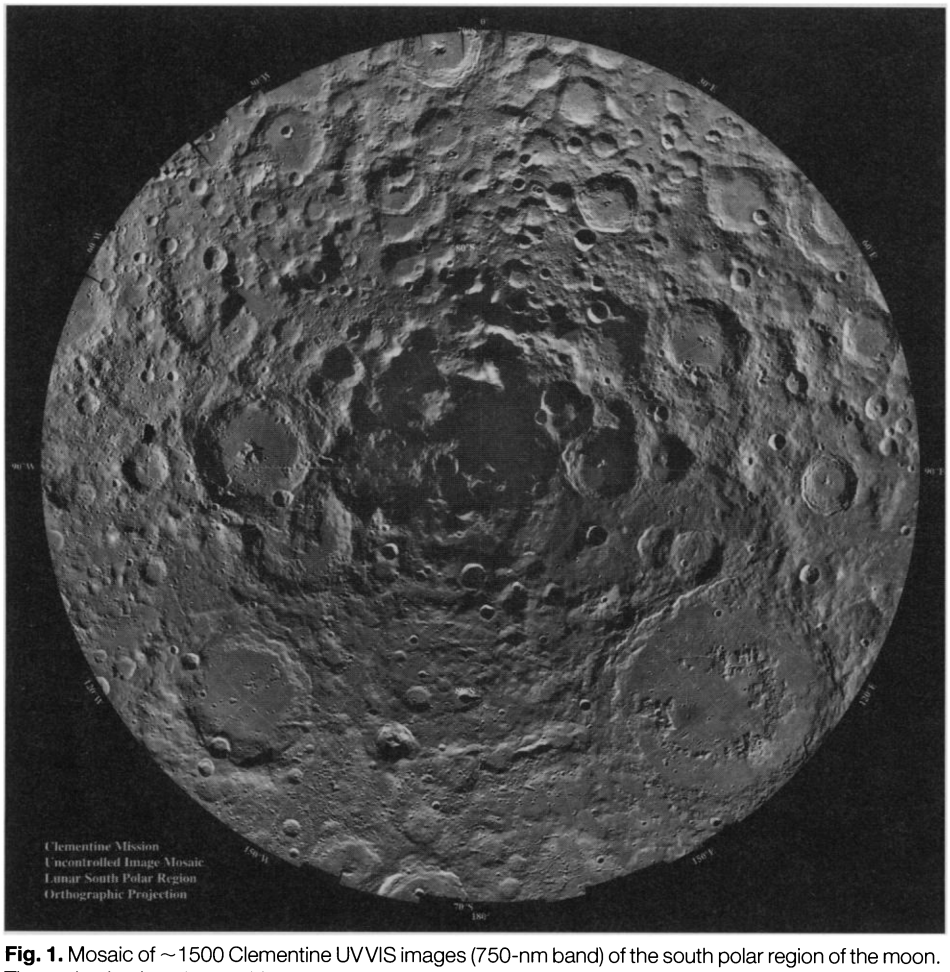

Fig. 1. Mosaic of ~1500 Clementine UVVIS images (750-nm band) of the south polar region of the moon. The projection is orthographic, centered on the south pole. The Schrödinger Basin (320 km in diameter) is located in the lower right of the mosaic. Amundsen-Ganswindt is the more subdued circular basin between Schrödinger and the pole.

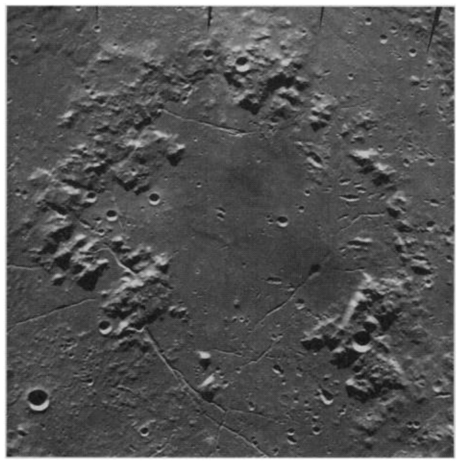

Fig. 2. Mosaic of UVVIS images (1000-nm band) of the central part of the Schrödinger Basin. The projection is orthographic, centered on the basin; total width of the mosaic is 216 km. Coordinates of the corners: upper left (71.1°S, 122.3°E); upper right (70.8°S, 144.1°E); lower left (78.3°S, 117.7°E); lower right (77.7°S, 152.1°E).

and a smooth facies (unit sp) with no discernible intrinsic relief, located chiefly in the inner basin within the peak ring. The smooth facies occupies most of the lowest parts of the basin and evidently was emplaced by rapid flow of the most-fluid shock-melted material. The melt has drained off the basin walls and peak ring, but a thin veneer of shock-melted material probably remains in patches on both the walls and the peak ring. A remarkable feature of the melt sheet is the occurrence of "ghost" craters, in both the rough and smooth facies, where preexisting small craters have been shallowly buried by the shock-melted material. These craters probably were formed by fragments ejected from Schrödinger on very high angle trajectories that landed in the basin before the melt accumulated in the low-lying areas of the basin. The late infall of high-angle ejecta at Schrödinger is analogous to that inferred at the 85-km-diameter crater Tycho (*10*). The presence of the ghost craters shows that the melt sheet is relatively thin, both in the annulus between the peak ring and the walls and also in the central basin. We see no haloed (dark or light) craters on the smooth plains unit (sp), which is consistent with an interpretation of locally derived materials. If unit sp were actually a blanket of foreign material (for example, Orientale ejecta), then excavation of true Schrödinger material from below this layer (superposed ejecta blankets) might exhibit an albedo contrast.

Near the center of the inner basin of Schrödinger is a low, lobate ridge measuring about 8 km by 24 km that is interpreted to have been formed by eruption of relatively viscous fluid (labeled r in Fig. 3). The ridged flow seems to have a lower crater density but is not readily discriminated in albedo or color from the smooth facies of the melt sheet. The ridge may have been formed by buckling of the melt sheet rather than by extrusion of a younger melt.

A deposit of dark eruptive material (labeled dm in Fig. 3) surrounds a volcanic vent on the east side of the inner basin. Localized along a northeast-trending graben, the 4.8 km by 8.6 km vent has a subdued raised rim typical of terrestrial maar volcanoes (*11*). It is one of the largest individual volcanic features with this form on the moon. The surrounding deposit partly fills the graben; it is several hundred meters thick at the rim of the vent (*12*) and thins to a feather edge at distances of 10 to 15 km from the vent. This unusual lunar volcano is very similar to but larger than several dark-halo craters localized along graben in the floor of Alphonsus, a large crater that was the target of the Ranger 9 lunar mission (*13*). Another similar volcano near the Rimae Sulpicius Gallus graben on the southwest edge of Mare Serenitatis is one of a series of vents that are the source of extensive dark mantling material (*7*). Spectrally similar dark deposits (*14*) were sampled directly by the Apollo 17 mission to the Taurus-Littrow valley, near the southeastern edge of Mare Serenitatis. They were shown to consist of pyroclastic basaltic glass (*7*). In the spectral bands of the UVVIS camera, the dark pyroclastic deposit around the Schrödinger maar is redder than the melt-sheet material (has a higher ratio of reflectance in the 750-nm versus the 415-nm band) but does not show the absorption feature near 1000 nm that is seen in the nearby flows of mare basalt (unit m). These three small patches of mare basalt occur in the northern part of the Schrödinger inner basin and appear to be located in or near the lowest parts of the basin floor. Their reflectance has an absorption band near 1000 nm, which is indicative of basaltic rocks of the maria elsewhere on the moon.

Ages can be assigned to the geologic units of the Schrödinger Basin by means of the density of superposed small craters, the superposition of the units themselves, and their relation to various swarms of secondary craters. On the basis of a small number of fairly large craters superposed on the Schrödinger Basin and its ejecta blanket, the basin was first assigned to the Nectarian System (*3*) and later reassigned to the younger Lower Imbrian Series (*7*). Using the Clementine south polar mosaic (Fig. 1), we made a careful count of all craters larger than 4 km in diameter that were superposed on Schrödinger and its ejecta blanket in the sector between 60°E and 150°W (Fig. 4). All secondary craters were rigorously excluded from this count. The cumulative crater frequency per square kilometer lies slightly below that for the Orientale Basin, except for a few craters larger than 30 km in diameter.

From these data alone, Schrödinger would appear to be slightly younger than Orientale, which would place the ejecta, the basin wall material, and the melt sheet in the Upper Imbrian Series. However, the difference in crater frequency between Schrödinger and Orientale is within the 1σ error for counting. Moreover, Wilhelms (*7*) noted a large secondary crater superposed on the northern ejecta blanket of Schrödinger that he identified as a probable Orientale secondary. We found a number of other post-Schrö-

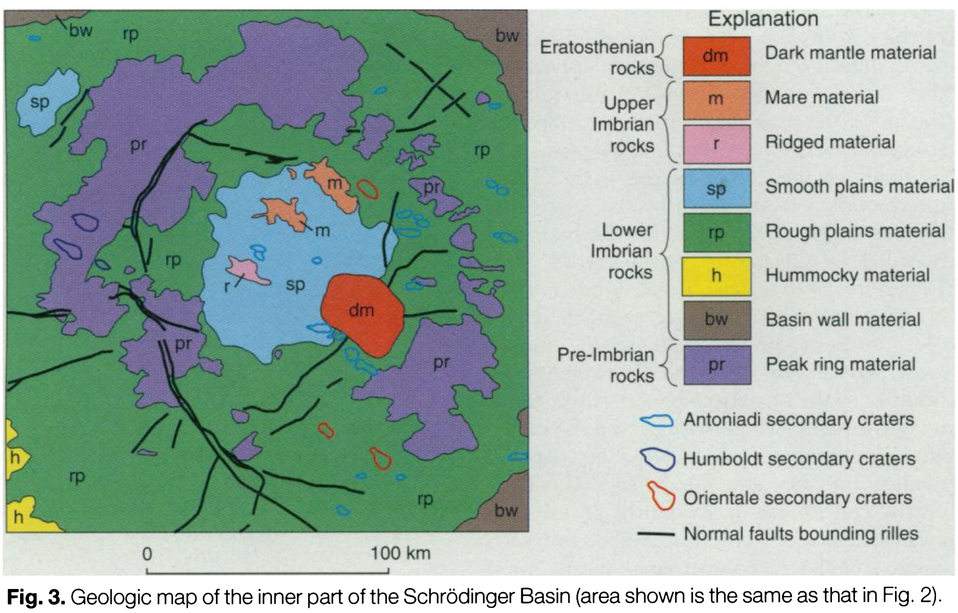

Fig. 3. Geologic map of the inner part of the Schrödinger Basin (area shown is the same as that in Fig. 2).

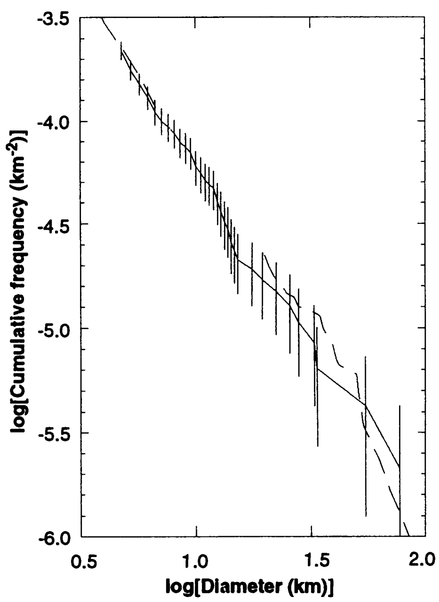

Fig. 4. Cumulative size-frequency distribution of primary craters on the Schrödinger Basin and its ejecta blanket (solid line) and on the Orientale Basin (dashed line). Distribution for the Orientale Basin is from Wilhelms (*7*). Vertical lines on Schrödinger curve indicate 1σ counting error.

dinger secondary craters in the south polar region that are probably part of the far-flung Orientale secondary crater swarm; some of them are delineated in Fig. 3. Hence, Schrödinger probably predates Orientale, although the two basins must be very close to the same age. Certainly, Schrödinger is one of the last two great impact basins to be formed on the moon. Because Orientale secondaries are superposed on them, the stratigraphic units related to Schrödinger should be assigned to the Lower Imbrian Series, the uppermost unit of which is defined to be the ejecta blanket of Orientale. On the basis of this stratigraphic correlation, the chronologic age of Schrödinger is close to 3.8 billion years (*7*).

Relatively large secondary craters that formed during two other impact events are also superposed on Schrödinger (Fig. 3). Some very elongate secondaries that cut the western peak ring are tentatively identified as part of the distant secondary swarm of the Late Imbrian protobasin Humboldt (207 km in diameter), which is ~50° of arc distant. Other large secondaries are related to the much nearer Late Imbrian protobasin Antoniadi (135 km in diameter), the south rim of which is shown at the edge of Fig. 1, near 170°W. As shown by the Clementine images, Antoniadi is surrounded by one of the densest secondary crater swarms found anywhere on the moon.

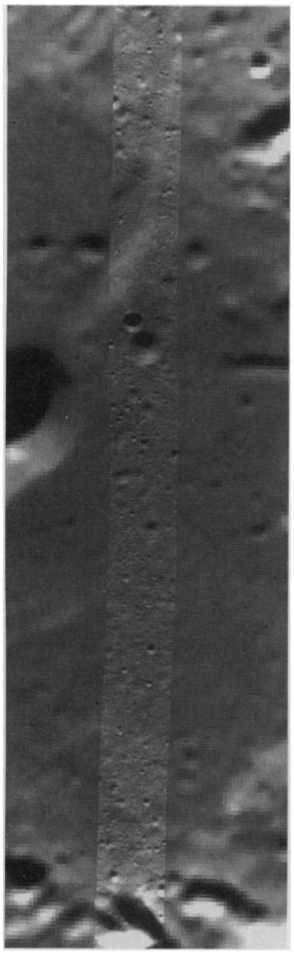

Fig. 5. Mosaic of Clementine high-resolution camera images (750-nm band) superimposed on UV-VIS image data (750-nm band) showing the eastern part of a maar-type volcano in the Schrödinger Basin. North is at the top, the width of UVVIS frame is ~12.4 km, and the width of high-resolution camera mosaic is ~2.9 km.

Mare basalt is superposed on the smooth facies of the melt sheet; locally it floods Antoniadi secondary craters. Strips of Clementine high-resolution images across both major patches of basalt reveal that the upper limit of the steady-state crater size distribution is about 300 to 400 m, in contrast with about 700 m for the melt sheet. This places the age of the basalt close to the Imbrian-Eratosthenian boundary, ~3.2 billion years old (*7*). We provisionally place the basalts in the latest Imbrian.

The dark pyroclastic deposit around the maar-type volcano in Schrödinger is superposed on a chain of small craters probably belonging to the Antoniadi swarm and postdates Antoniadi. Images taken with the Clementine high-resolution camera (Fig. 5) reveal the population of craters down to 10 m in diameter formed on the maar rim. The degradation of these small craters gives an upper limit of the steady-state crater size distribution of about 100 m. This places the age of the maar in the late Eratosthenian, at ~1 to 2 billion years old (*7*). Because these small craters are formed on a deposit presumed to be unconsolidated or weakly consolidated ash, where impact cratering efficiency may be substantially higher than on most other materials on the lunar surface, it is possible that the maar is Copernican in age (<~1 billion years old).

A striking pattern of graben that offset the rocks of the peak ring and the melt sheet in Schrödinger (Figs. 2 and 3) provides a clue to the ancient stress field and the origin of the deformation. The graben tend either to be aligned roughly radially with respect to the center of the basin or to roughly follow the arc of the peak ring. This is a pattern of structural extension that could be produced by uplift of the center of the basin. This interpretation is supported by the relatively shallow depth (2 to 3 km) for the basin as revealed by Clementine altimetry (*4*, *8*). Departures from a strict radial or circumferential pattern probably are controlled by old, pre-Schrödinger faults in the lunar crust. We suggest that the faulting is the result of slight isostatic rebound of the center of the basin that perhaps occurred shortly after emplacement of the melt sheet. Antoniadi secondaries appear to be superimposed on the graben system. Evidently, an impact basin the size of Schrödinger does not become completely compensated during the early collapse of the transient impact cavity and formation of the peak ring but may approach this state by slow, quasi-viscous flow of the crust and mantle.

The eruption of the maar along one of the graben in Schrödinger is consistent with the occurrence of similar volcanoes along circumferential graben around basin-filling maria and in large craters elsewhere on the moon (*15*). The fracture systems associated with these graben evidently reach deep enough to tap or intersect other fractures that tap comparatively volatile-rich regions in the lunar mantle. The Schrödinger maar appears to be younger than others previously described (*15*). This suggests that the center of Schrödinger may have remained under tension for much of lunar history.

REFERENCES AND NOTES

1. S. Nozette *et al.*, *Science* **266**, 1835 (1994).
2. J. E. Westphall, *Assoc. Lunar Planet. Obs. J.* **34**, 149 (1990); *Sky Telesc.* **82**, 556 (1991).
3. D. E. Wilhelms, K. A. Howard, H. G. Wilshire, *U.S. Geol. Surv. Map I-1162* (1979).
4. P. D. Spudis, R. A. Riesse, J. J. Gillis, *Science* **266**, 1848 (1994).
5. K. Watson, B. C. Murray, H. Brown, *J. Geophys. Res.* **66**, 3033 (1961); J. R. Arnold, *ibid.* **84**, 5659 (1979); A. P. Ingersoll, T. Svitek, B. C. Murray, *Icarus* **100**, 40 (1992).
6. N. J. S. Stacy, thesis, Cornell University (1993).
7. D. E. Wilhelms, *U.S. Geol. Surv. Prof. Pap. 1348* (1987).
8. M. T. Zuber *et al.*, *Science* **266**, 1839 (1994).
9. D. J. Roddy, R. O. Pepin, R. B. Merrill, Eds., *Impact and Explosion Cratering* (Pergamon, New York, 1977); R. A. F. Grieve, P. B. Robertson, M. R. Dence, in *Proceedings of the Conference on Multiring Basins: Formation and Evolution*, P. H. Schultz and R. B. Merrill, Eds. (Pergamon, New York, 1981); H. J. Melosh, *Impact Cratering: A Geologic Process* (Oxford Univ. Press, Oxford, 1989). The proof that central peaks of large impact craters are derived by uplift of the floors of the transient cavities comes from study of well-explored terrestrial impact structures such as Gosses Bluff (Northern Territory, Australia) and the Manson impact structure (Iowa), where the structural uplift can be accurately determined.
10. E. M. Shoemaker *et al.*, in *NASA Spec. Publ. 173* (1968), p. 13.
11. ———, in *Physics and Astronomy of the Moon*, Z. Kopal, Ed. (Academic Press, New York, 1962). The similarity between the crater in Schrödinger and terrestrial maars does not imply a phreatomagmatic eruption on the moon. On the contrary, ejection velocities of the pyroclastic material much lower than those required on Earth will produce craters with maar-type form on the moon [see J. W. Head and L. Wilson, *Proc. Lunar Planet. Sci. Conf.* **10**, 2861 (1979)].
12. The thickness of the pyroclastic deposit of the rim was estimated by determining the depth of the unfilled part of the graben from shadow measurements.
13. R. L. Heacock, *Jet Propul. Lab. Tech. Rep. 32-800* (1966), p. 7.
14. L. R. Gaddis, C. M. Pieters, B. R. Hawke, *Icarus* **61**, 461 (1985).
15. C. R. Coombs and B. R. Hawke, in *Proceedings of the Kagoshima International Conference on Volcanoes*, Kagoshima, Japan (1988), pp. 416–419; C. R. Coombs, thesis, Univ. of Hawaii, Honolulu (1988); B. R. Hawke *et al.*, *Proc. Lunar Planet. Sci. Conf.* **19**, 255 (1989); C. R. Coombs and B. R. Hawke, *ibid.* **22**, 303 (1992).

16. We thank C. Acton, H. Taylor, L. Perez, J. Eliason, K. Edwards, K. Becker, D. Cook, and A. Bennett for their technical contributions without which this work would not have been possible.

24 August 1994; accepted 25 October 1994